——————— *Review* ———————

Recent Study on the Mechanism of the Electrodeposition of Iron-group Metal Alloys

Tetsuya AKIYAMA and Hisaaki FUKUSHIMA

Department of Materials Science and Engineering, Faculty of Engineering, Kyushu University, Hakozaki, Higashi-ku, Fukuoka, Fukuoka-ken, 812 Japan.

Almost 300 kinds of binary alloys have been electroplated so far to modify surface properties of substrates. Electrodeposition of iron-group metal alloys has been studied most intensively for last 16 years. This trend was caused not only by the excellent properties of the coatings that were useful for many industrial applications but also by the fact that their electrodeposition behavior was interesting from an academic point of view. This review correlates the mechanism proposed so far to explain the abnormal electrodeposition behavior of iron-group metal alloys.

KEY WORDS: mechanism; alloy deposition; iron-group metals; anomalous type; induced type.

1. Introduction

Electroplating has been conducted mainly to modify certain surface properties of the substrate. Of functions to be provided, good surface appearance, corrosion and wear resistance are basically important. These properties could be improved significantly by alloy plating. Alloy deposition has a 150 year long history that goes back to brass plating by Jacobi in 1841, and attempts have been made so far to electrodeposit 292 kinds of binary alloys from aqueous solutions as shown in **Table 1**.[1,2] Approximately 90 kinds of alloys, almost one third of those reported previously, contain iron-group metal, and almost 20% of whole alloys reported contain Au or Ag. The number of reports on binary alloy deposition between 1975 and 1990 is summarized in **Table 2**, showing that the number of reports amounts to 1127 for iron-group metal alloys, 207 for Au or Ag alloys and 147 for solder (Sn–Pb) alloys. Thus, the electrodeposition of these alloys has been conducted most frequently because the coatings show an outstanding favorable property for practical use. Among the iron-group metal alloys, the alloys with Zn have been investigated most actively, which was resulted from the frantic research by steel manufacturers to develop highly corrosion-resistant alloy plated steel sheet for automotive body panels.[3-5] The mutual alloys of iron-group metals have been electroplated to employ mainly their magnetic properties[6-15] as well as to substitute the conventional decorative plating of Ni.[16-25] Electroplating of other alloys presented above were for surface finishing of electric contacts or mechanical parts, *etc.*, as well as for decorative purposes.

The condition that permits alloy deposition is described by following equation consisting of four terms.

$$(E_M^0 - E_N^0) + (RT/nF)\ln(a_M^{n+}/a_N^{n+})$$
$$- (RT/nF)\ln(a_M/a_N) - (\eta_M - \eta_N) = 0$$

The first term is the difference in standard single electrode potential between the metals in which M is more noble than N. The second and third are related to the activity of metals in bath and in deposit. The fourth indicates the difference in deposition overpotential between the metals. R, T, n and F are gas constant, temperature in Kelvin, valence of each metal ion in bath and Faraday constant, respectively. The first term $(E_M^0 - E_N^0)$ is unequivocally determined when metals to be codeposited are specified, and is positive because M was assumed to be more noble than N. The other terms differ in magnitude when bath compositions or plating conditions are varied. When these terms are varied to cancel the first term, the equation is satisfied to permit alloy deposition. In Sn–Pb system, the first term is so small (0.012 V) that the equation is easily satisfied by alternating the metal ion concentration ratio in bath, resulting in obedient alloy deposition even from simple acidic baths. In alloy systems containing Au or Ag, the first term is often much larger than 1 V. Therefore, these alloys are preferably obtained from cyanide baths where more noble Au or Ag forms stable complex ion to reduce greatly its activity in bath as well as to increase deposition overpotential. On the other hand, most iron-group metal alloys such as Ni–Zn or Fe–Ni is deposited from sulfate or chloride baths where each metal exists in its simplest form of hydrated ion. The difference in standard single electrode potential between Ni and Zn, for example, is about 0.5 V, which is too large to be canceled only by the alteration of metal ion concentration ratio in bath. In this case, however, the alloys are actually deposited at high current efficiency under limiting current density

Table 1. Binary alloys electroplated up to 1960 (■), up to 1970 (●), up to 1982 (▲) and up to 1990 (★). Data surveyed lately were added to Refs. 1 and 2).
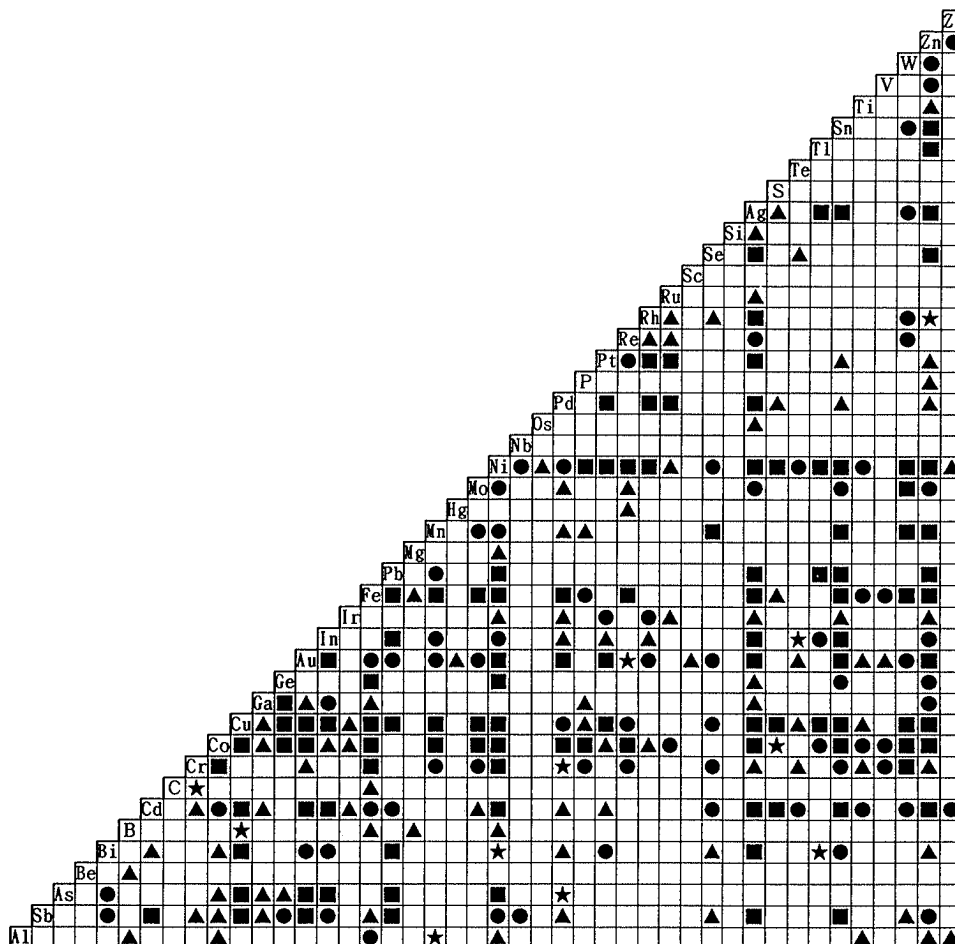
(Table 1 is a large upper‑triangular matrix of the elements whose diagonal labels read, from the lower‑left corner upward/to the right: Al, Sb, As, Be, Bi, B, Cd, C, Cr, Co, Cu, Ga, Ge, Au, In, Ir, Fe, Pb, Mg, Mn, Mo, Ni, Nb, Os, Pd, P, Pt, Re, Rh, Ru, Sc, Se, Si, Ag, S, Te, Tl, Sn, Ti, V, W, Zn, Zr. Each cell is marked with ■, ●, ▲ and/or ★ according to the legend above.)

Table 2. Number of reports on binary alloy deposition since 1975 up to 1990.

	Mo	W	Mn	Re	Pd	B	Ga	In	C	Ge	Pb	P	Sb	Bi	S
Cr	13	7	1	1	1				1						
Sn			1		4			3			147		1	14	
Cu	16		1	3	1			2			5	1		5	
Ag	3	6			14		3	2		1				9	
Au	9	13	8	1	10			.1							
Cd	7	4	11	3	1			1			3		5	1	
Zn	12	3	62		17		1	12	1	1	3		1		
Fe	128		10	1	2			4	1				1		
Co	10	40	19	6	3			3			3		3	5	1
Ni	50	118	64		5	6		47	10		8		2		8

Additional inter‑element (iron‑group) pairs shown in the shaded left columns include, among others, Co–Fe ≈ 67 (anomalous), Ni–Co ≈ 209 (anomalous), together with Fe–Zn, Fe–Cd, Co–Zn, Co–Cd, Ni–Zn, Ni–Cd (anomalous) and Ni–P (induced).

▨ : anomalous codeposition, ■ : induced codeposition

for each metal deposition. This suggests that the first term of the equation should be canceled either by reduced activity of less noble Zn in deposit or by increased deposition overpotential of more noble Ni due to certain factors other than diffusion control. Further, less noble Zn codeposits preferentially with more noble Ni and is called anomalous codeposition. It is well known that the anomalous codeposition also appears in the iron-group metal alloys with Cd and the mutual alloys of iron-group metals. Another type of anomaly furthermore appears in the electrod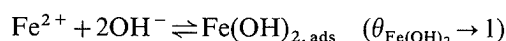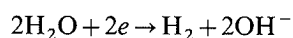eposition of iron-group metal alloys. The reluctant Mo or W, which cannot be deposited by itself from aqueous solutions, codeposits with inducing iron-group metals, which is called induced codeposition.

Besides the industrial importance, these anomalies appearing in the electrodeposition of iron-group metal alloys have been arousing an academic interest. This is another reason for the largest number of report concerning with iron-group metal alloy deposition. The mechanisms proposed so far to explain the anomalies are reviewed below in the Fe–Ni, iron-group metal–Zn and iron-group metal–Mo, W or P systems in that order.
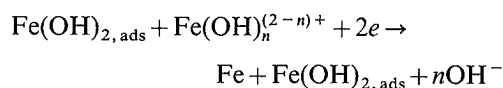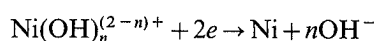
2. Anomalous Codeposition

2.1. Fe–Ni System

The most plausible hypothesis for Fe–Ni alloy deposition is the hydroxide suppression mechanism proposed originally by Dahms and Croll.[26,27] A mathematical equation was derived to evaluate the pH changes in the cathode layer due to hydrogen evolution during electrolysis. The polarization curves measured using rotating disc electrode for alloy and each metal depositions suggested that Ni deposition was strongly suppressed in the presence of Fe at relatively less noble potentials (**Fig. 1**). The Ni deposition began to be suppressed when the metal hydroxide was formed on the cathode at the potential corresponding to the diffusion limiting current for hydrogen evolution. Since no suppressed Ni deposition was observed in the single deposition of Ni, the formation and subsequent preferential adsorption of ferrous hydroxide were concluded to cause the suppressed Ni deposition, although the hydroxides of both Fe and Ni were formed when the limiting current of hydrogen was exceeded. The mechanism proposed was described as follows.

$$2H_2O + 2e \rightarrow H_2 + 2OH^-$$

$$Fe^{2+} + 2OH^- \rightleftharpoons Fe(OH)_{2,ads} \quad (\theta_{Fe(OH)_2} \rightarrow 1)$$

at θ

$$Fe(OH)_{2,ads} + Fe(OH)_n^{(2-n)+} + 2e \rightarrow$$
$$Fe + Fe(OH)_{2,ads} + nOH^-$$

at $1-\theta$

$$Ni(OH)_n^{(2-n)+} + 2e \rightarrow Ni + nOH^-$$

Many reports published later[28-34] supported the hydroxide suppression mechanism. Using moving cylindrical wire cathode in chloride–sulfate baths, Bielinski and Przyluski[28] found that an increase in current density reduced the Fe content in deposits and
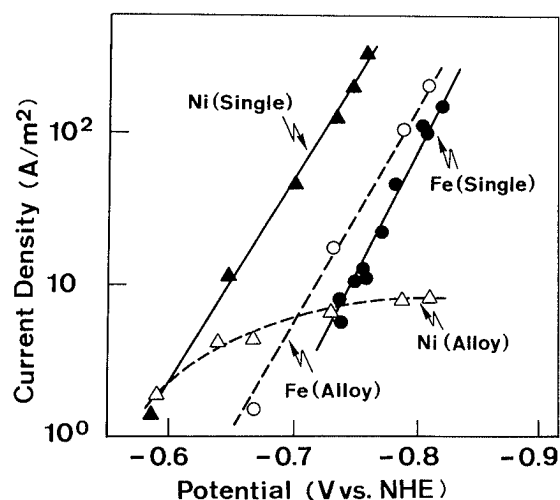
increased in the cathode current efficiency since the Ni deposition rate was controlled by charge transfer while the rate for Fe and hydrogen depositions was diffusion controlled. They also suggested that the strong adsorption of hydrated Fe compounds on the cathode brought about the large polarization for alloy deposition in the presence of Fe^{2+} in bath and that the surface concentration of these compounds was varied depending on the Fe^{2+} concentration or pH of the bath.

Using disc electrode, Horkans[30,31] found the maximum Fe content in deposits from sulfate, chloride or their mixed solutions at a certain current density, and explained as follows. At low current densities where the pH rise in the cathode layer was small, little iron hydroxide formed to make the Ni content relatively high. Increasing current density brought about a larger pH rise, resulting in the increased Fe content. Then the Fe content decreased at higher current densities. Because the partial current density of Fe was well below its diffusion limiting current at the maximum Fe content, the decrease in Fe content was not caused solely by mass transport limitation of Fe^{2+} in solution. It was concluded that the decrease in Fe content at high current densities was resulted from the slow ionic diffusion in ferrous hydroxide through which Fe^{2+} discharge took place. Horkans also recognized that chloride ion increased the current efficiency and decreased Fe content. Catalyzing effect of the chloride ion and difference in H^+ ion diffusiveness were taken into account to explain the higher current efficiency, while weak complexation to prevent ferrous hydroxide formation accounted for the lower Fe content.

Attempts[29,32-34] have been made to indicate empirically the pH rise at the surface predicted by Dahms and Croll.[26,27] Using specially designed glass microelectrode, Beltowska-Lehman and Riesenkampf[29] evaluated the pH near the rotating disk electrode. The results showed the sufficient alkalization for the formation of iron hydroxide, which confirmed the hydroxide suppression mechanism.

Another study was made both experimentally and theoretically to clarify the relation between the anomalous codeposition of Fe with Ni and the pH change near the cathode by Koura and Yasuda[32,33] (**Fig. 2**). For the electrodeposition of Fe or Ni, the pH change estimated using Dahms' equation[27] was consistent with that measured using Sb microelectrode technique. The anomaly appeared only when the pH in the cathode layer raised up to neutral value enough to form $Fe(OH)_{2,ads}$, and not only the polarization of Ni deposition but also the depolarization for Fe deposition due to $Fe(OH)_{2,ads}$ brought about the preferential deposition of less noble Fe. A decrease in the double layer capacitance was also recognized, which was probably due to the formation of metal hydroxide during electrolysis.

Periodically reversed current electrolysis retarded the preferential deposition of less noble Fe,[35,36] because the adsorbed hydrogen atom, which was formed during cathodic period, was oxidized during anodic period, preventing the pH rise in the cathode layer.

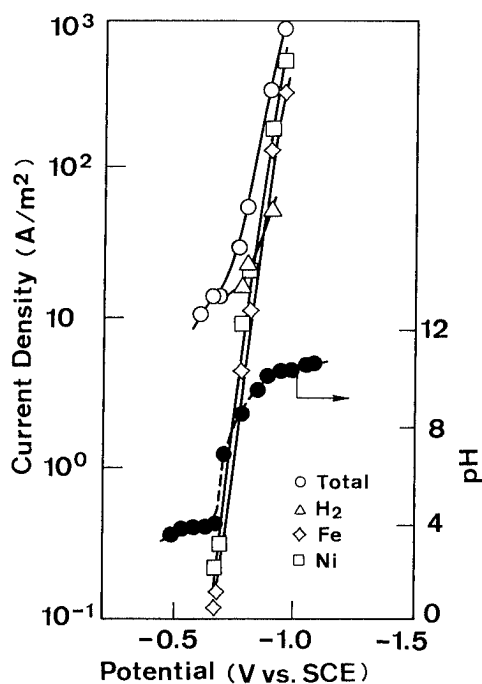On the other hand, Romankiw[37] insisted the presence

Fig. 1. Partial polarization curves of Fe and Ni in single and alloy deposition.[27]

Ni plating bath: $NiSO_4$ 0.5 mol/L, H_2SO_4 0.01 mol/L
Fe plating bath: $FeSO_4$ 0.5 mol/L, H_2SO_4 0.01 mol/L
Alloy plating bath: $NiSO_4$ 0.5 mol/L, $FeSO_4$ 0.5 mol/L, H_2SO_4 0.01 mol/L

© 1992 ISIJ

Fig. 2. Total and partial polarization curves for Fe–Ni alloy deposition and pH in vicinity of cathode.[33] Bath composition: $NiSO_4$ 0.18 mol/L, $FeSO_4$ 0.04 mol/L, pH 3.0

Fig. 3. Schematic illustration of initial composition gradient in electrodeposited Fe–Ni alloys.

of ferric hydroxide during anomalous codeposition. The pH in the cathode layer was evaluated using flat bottom glass electrode coupled with screen mesh cathode. From the results that the pH in the cathode layer was harder to rise in Fe solution than Ni solution and that the solubility constant was much larger in $Fe(OH)_2$ and $Ni(OH)_2$ than in $Fe(OH)_3$, it was postulated that precipitation of ferric hydroxide should play an important role not only in the buffering action especially in the cathode layer but also in the codeposition process of Fe–Ni alloys.

Similar mechanism was proposed by Bielinski and Przyluski,[38] who demonstrated that the introduction of Fe^{3+} to the solution increased the cathodic polarization and reduced the cathode current efficiency for alloy deposition, suggesting that the formation of adsorbed ferric hydroxide layer caused the decrease in deposition rate of Ni^{2+}.

Hessami and Tobias[39] developed the mathematical model based on the existence of $FeOH^+$ and $NiOH^+$ which were reportedly involved in each metal deposition[40,41] and had much larger dissociation constant than each corresponding metal hydroxide. The surface concentration of various species involved in the alloy deposition was calculated to show that their model could predict well such salient features of anomalous codeposition like the preferential deposition of less noble Fe and the appearance of maximum Fe content. Moreover, the effects of agitation and pH on the alloy deposition were simulated. The results were qualitatively in good agreement with the experimental observations.[42] According to their mechanism, the retarded Ni deposition was explained by the relative concentration of both metal-hydroxide ions. The coverage of $FeOH^+$ was
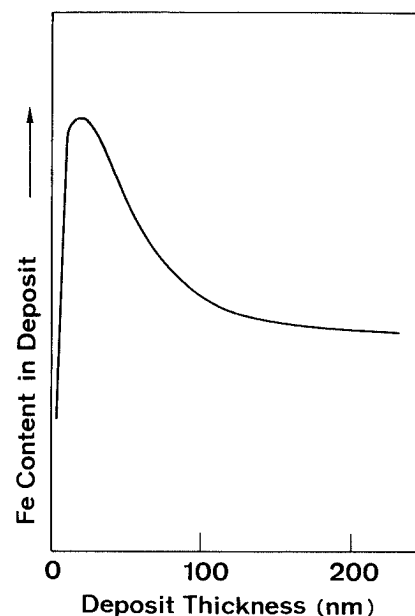
higher than $NiOH^+$ because of its much smaller dissociation constant. Presence of $FeOH^+$ ions had two consequences: (1) $FeOH^+$ ions competed with $NiOH^+$ for surface sites, and (2) the pH rise at the surface was somewhat buffered, causing lower coverage of $NiOH^+$ compared with that in pure Ni deposition. Subsequently, Ni deposition was inhibited in the presence of Fe.

Lieder and Biallozor[43,44] proposed another mechanism of anomalous codeposition, in which no metal-hydroxide was involved. It was found in the chloride solutions of various buffer capacities that the ratio of Fe to Ni in the alloy was always higher than in the electrolytes irrespective of the buffer capacity, which was hardly explained by Dahms' model.[26,27] In their opinion, Ni^{2+} was discharged at first to form very thin Ni film on which water molecules chemisorbed to form $Ni(OH)_{ad}^+$. From the competition between Ni^{2+} and Fe^{2+} ions to occupy the active sites, the preferential deposition of Fe and the hindrance of Ni^{2+} discharge rate were resulted.

Besides the preferential deposition of less noble metal, the electrodeposition of Fe–Ni alloys has been found to have another characteristic feature of the significant composition gradient in the first several hundreds nanometers of electrodeposits[45–51] (Fig. 3). This has been the fatal disadvantage especially in the application to the magnetic devices. On the basis of hydroxide suppression mechanism,[26,27] the occurrence of composition gradients at the initial stage of alloy deposition was interpreted in the following way[46,48]:

(1) Initial deposition of Ni—Ni will plate out preferentially until the hydrogen ion concentration at the surface is depleted to form metal hydroxide;

(2) Subsequent enrichment in Fe—When the adsorption of hydroxides has taken place, ferrous ions from the diffusion layer are discharged preferentially;

(3) Approach to equilibrium composition—The ferrous ions are depleted in the diffusion layer and

steady-state diffusion conditions for ferrous ions are completed.

On the basis that the initial compositional change occurs when only Fe deposition rate is controlled by diffusion, Dahms[48] calculated theoretically the composition gradients under galvanostatic and potentiostatic conditions to compare them with the experimental data. The lower Fe content was observed experimentally and this trend was concluded to be caused by the formation of ferrous hydroxide at the cathode surface which would lower the amount of ferrous ions available for deposition.

Several attempts have been made to eliminate the initial composition gradient in deposited Fe–Ni alloys. For instance, it was presented that the composition profile of the alloy films deposited potentiostatically was relatively constant.[43,51] According to Eastham et al.,[49] no composition gradient was found in the alloys produced at relatively more positive potentials than -1.0 V vs. SCE at which a diffusion layer was formed quickly and from then on remains at constant composition throughout the plating time. It was also indicated that the deposition at pulsed potentials yielded the flattest composition–thickness curves so far achieved. Omata et al.[22] reported that a constant composition and precise control of a few micrometers in thickness of the films were attained by applying instantaneous high current density prior to a steady plating stage to hasten the increase in the pH in the cathode layer.

2.2. Zn–Iron-group Metal System

Although many attempts have been made to explain the anomalous codeposition of Zn with iron-group metals, the hydroxide suppression mechanism is most plausible, as is the case of Fe–Ni system. Brenner[52] pointed out the existence of transition current density at which the codeposition behavior changed from the normal to the anomalous type and the considerable suppression of Ni deposition occurred in the presence of Zn (**Fig. 4**). Since the effect of Zn on the Ni deposition was similar to that of certain addition agents, he proposed a hypothesis referred to as the "addition agent theory". When the current density was sufficiently high
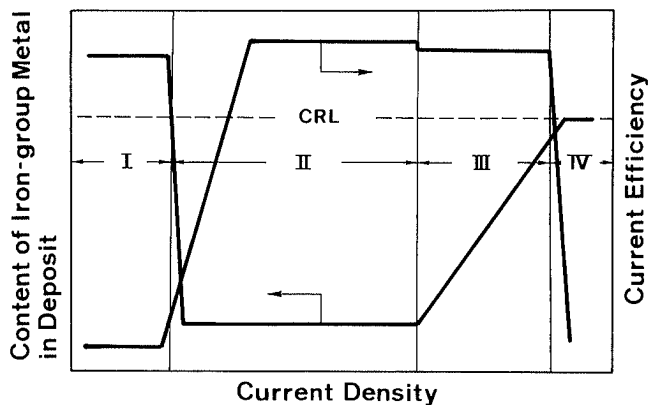
to raise the pH of the cathode diffusion layer significantly, the "addition agent" such as hydrous oxide or hydroxide of Zn was produced by the cathodic reaction. The transition current density would appear, owing to the requirement of a certain critical concentration of the "addition agent" in the cathode diffusion layer.

Knoedler et al.[53-55] also found that the polarization behavior for Ni or Co deposition from Watts type baths containing Zn was just the same as in the presence of organic inhibitors such as butindiol and N-methylphthaleneimid. This was caused by the strong inhibition due to the Zn hydrolysis products for Ni or Co deposition. It was also found that Zn deposition took place more readily with preceding $Zn(OH)^+$ or $Zn(OH)_2$ formation than in direct discharge of Zn^{2+} ions.[56]

Higashi and Fukushima[57-68] have been conducting the fundamental studies on the electrodeposition of Zn–iron-group metal alloys from sulfate solutions. The alloy deposition behavior was divided with respect to the current density into the following four segments (Fig. 4): region I where the normal type alloy deposition occurred with poor current efficiency; region II where the preferential deposition of less noble Zn proceeded at relatively high current efficiency and the alloy composition hardly tended to change; region III where the iron-group metal content of the alloy steadily increased while acceptably high current efficiency was still remained; and region IV where the iron-group metal content of alloy increased to reach the metal-percentage of iron-group metal in the solution but current efficiency decreased greatly. The boundary current density between regions I and II, which has been so called the transition current density, was proportional to the buffering capacity of the electrolyte used, and the boundary current densities between regions II/III and III/IV were related to the limiting current of Zn and iron-group metal,
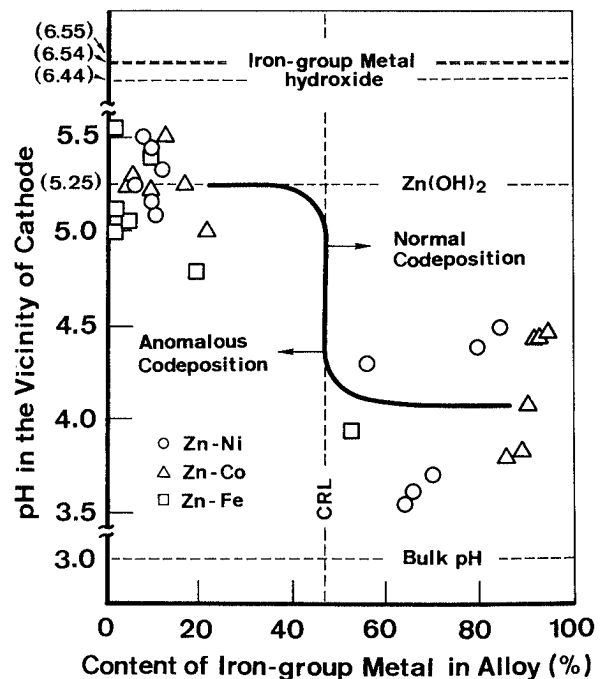

Fig. 4. Schematic illustration of dependences of alloy composition and cathode current efficiency on current density in electrodeposition of Zn–iron-group metal alloys. The boundary current density between regions I and II corresponds to transition current density.

Fig. 5. Relationship between alloy composition and pH in vicinity of cathode during electrodeposition of Zn–iron-group metal alloys.[60]

respectively.[63-66,68] They demonstrated using Sb microelectrode technique that the pH in the cathode layer increased to the critical pH for $Zn(OH)_2$ precipitation during anomalous codeposition[59,60] and supported the hydroxide suppression mechanism (**Fig. 5**). Among the ions which are capable of being discharged, Zn begins to deposit at its equilibrium potential, whereas iron-group metals have the inherent property of not beginning to deposit at their equilibrium potentials but requiring an extra overpotential due to substantially limited number of deposition site on the cathode. Therefore, the deposition of iron-group metal is further suppressed easily by the adsorption of Zn hydroxide on the deposition sites for iron-group metals, resulting in the preferential deposition of Zn.

Some investigators also evaluated the pH change at the cathode in sulfate solutions using Sb microelectrode technique.[69,70] Shibuya and Kurimoto[69] observed the pH rise in the cathode layer at higher current densities in Zn–Ni system, and suggested that the change in relative deposition rates of Ni and Zn, resulted from thickness change of Zn hydroxide film, affected the composition and hence the phase structure of deposited alloys. Fajadro et al.[70] found that the alloy was substantially obtained when enough alkalization of the cathode layer occurred to precipitate Zn hydroxide, and that the pH in the cathode layer was significantly affected by the concentration of the sulfuric acid in solution and by agitation.

If the anomalous codeposition of Zn–iron-group metal proceeds along with the hydroxide suppression mechanism, Zn hydroxide might be included in the deposits.[71,72] Tsuru et al.[72] quantitatively analyzed Zn in deposits not only by atomic absorption spectrometry but also by anodic chronoamperometry, to evaluate separately the amount of Zn hydroxide and metallic Zn in Zn–Ni alloys potentiostatically deposited from the sulfate solutions (**Fig. 6**). The results showed that the content of Zn hydroxide in deposits was closely related to the rate of hydrogen evolution and hence the pH rise in the cathode layer during alloy deposition.

In chloride solutions, the electrodeposition behavior of Zn–iron-group metal alloys tended to change from the anomalous to the normal type with an increase in the concentration of NaCl, KCl or NH_4Cl in baths.[73-75] This trend was explained by the changes in the structure and composition of Zn hydroxide in the presence of Cl^- ion,[73] catalyzing effect of Cl^- ion for the deposition rate of iron-group metals,[65] or by the retarded Zn hydroxide formation rate due to K^+, Na^+ and NH_4^+ ions.[74]

Several mechanisms free from Zn hydroxide formation, on other hand, are also available. Yur'ev and Volkov[76] measured the polarization curves for separate or simultaneous deposition of Ni and Zn from sulfate solutions. They postulated that the polarization of Ni deposition in the presence of Zn was evidently attributable to two factors; (1) the high overvoltage of Ni deposition on Zn and (2) the structural peculiarities of the electric double layer when Ni and Zn ions coexisted in the solution.

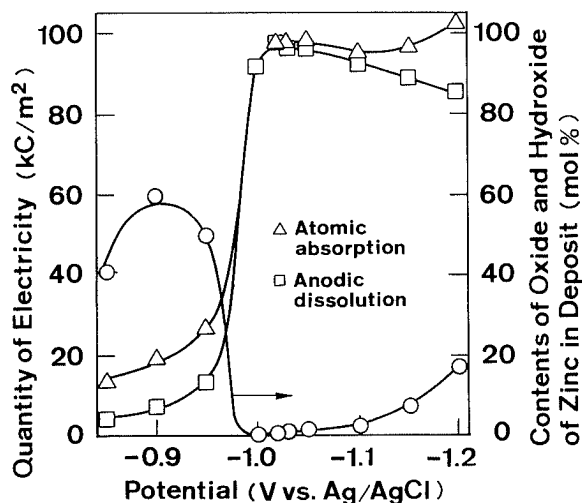Felloni et al.[77] concluded in the Zn–Ni alloy de-

Fig. 6. Cathode potential-dependence of quantity of electricity determined by atomic absorption spectrophotometry and by anodic chronoamperometry. The quantity difference gives the amount of oxidized Zn in deposits. The content of oxide and hydroxide of Zn in deposits is also shown in the figure.[72]

Bath composition: $NiSO_4$ 0.2 mol/L, $ZnSO_4$ 0.5 mol/L, H_3BO_3 0.32 mol/L, NH_4Cl 0.26 mol/L, Na_2SO_4 1.07 mol/L, pH 4.0

position from chloride solutions that the hydroxide suppression mechanism was valid only in particular plating conditions that yielded unsatisfactory alloys probably containing hydroxides. The most likely explanation for the anomalous codeposition might be that extremely lower values of the exchange current densities of iron-group metals than Zn were so favorable that they canceled the thermodynamic nobleness of these metals with respect to Zn.

From the different standpoint, an alternative mechanism for the anomalous codeposition was suggested by Nicol and Philip[78] in connection with the underpotential deposition. When less noble metal was deposited onto more noble metal substrate, the potential required for monolayer deposition was different from that for bulk metal deposition, and the potential difference was closely related to the difference in work function between the metals. Provided that the work function of deposited alloys lay in an intermediate level between the constituents, the continuous underpotential deposition of less noble metal was allowed to permit preferential deposition of Zn.

A mathematical model for the kinetics of Zn–Ni alloy deposition on the rotating disk electrode has been established by Mathias and Chapman.[79-82] Their aim was to predict the deposit composition and thickness distribution over a wide range of plating conditions in practical cells of any geometry. The calculation of surface species concentration revealed that the anomalous codeposition occurred even when the hydrogen current was never large enough to raise the interfacial pH much higher than that in the bulk. Rather, the results suggested that the anomalous deposition should be attributed simply to the fact that the exchange current density of Zn was in five orders of magnitude higher than that of

Ni and the facile Zn was kinetically deposited much more rapidly than the sluggish Ni at practical total current densities.

Kurachi et al.[83-88] investigated actively the electrodeposition behavior of Zn–Ni alloy from sulfate solutions in relation to the alloy composition and its phase. It was found that the electrodeposited Zn–Ni alloys were composed of three major phases, α, γ and η (Fig. 7). The alloys consisting of single γ phase were stably obtained in a wide range of bath composition although the phase composition strongly depended on the deposition potential.[83,84] The Gibbs free energy for the formation of electrodeposited alloys was found to be most negative when γ phase was predominantly deposited from the solutions of various compositions.[85] This was consistent with the fact that the alloys consisting of single γ phase showed the best corrosion performance[89] and its deposition potential was more positive than pure Zn.[72] As for the mechanism of Zn–Ni alloy deposition, it was shown that there was no interaction between Ni and Zn ions[86] in electrolyte. The interfacial impedance measurement during electrolysis[87] indicated the increase in double layer capacitance, which was not consistent with the prediction of so-called "addition agent theory".[52] It was concluded that Zn^{2+} was concentrated in the double layer region to form an intermediate polynuclear complex, $[4Zn(OH)_p Ni(OH)_q]^{m+}$ ($0<p$, $q>2$, $m<10-4p-q$), which had similar structure to γ phase.[88]

Swathirajan[90,91] applied the potentiodynamic and galvanostatic stripping techniques for the characterization of Zn–Ni phases and their deposition process onto the rotating disk electrode. He also found that the phase composition of the alloys varied with the deposition potential, and estimated the equilibrium potentials of α, γ and η phases. While the equilibrium potential of γ and η phases were about 90 and 20 mV more positive, respectively, than that of bulk Zn, α phase had extremely more positive equilibrium potential with respect to bulk Zn by about 360 mV, indicating the occurrence of under potential deposition of Zn. It was pointed out that the
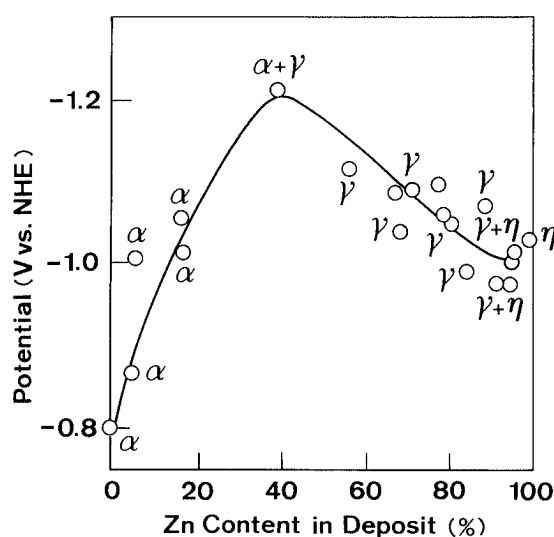
hydroxide suppression mechanism hardly explained why a strong inhibition of Ni deposition was observed even in the normal region before any appreciable Zn deposition began. The fact that the rotation of the electrode decreased the transition current density was not also explicable satisfactorily by the hydroxide suppression mechanism, since the rotation should prevent the pH rise at the surface to increase the current density for oxide film formation. On the basis of the theoretical and experimental results, Swathirajan considered the anomalous codeposition of Zn–Ni was caused by two factors; (1) the differences in the exchange current density between two metals and (2) the inhibition of Ni deposition due to underpotentially deposited Zn.

3. Induced Codeposition

3.1. Mo (W)–Iron-group Metal System

Owing to the distinct properties, the Mo or W alloys with iron-group metals have been of special interest in the practical plating.[92-109] On the other hand, the electrodeposition of Mo (W)–iron-group metal alloys belongs to the induced type, and therefore the codeposition behavior is complicated. Effects of plating variables on the composition of Ni–Mo alloy and on the cathode current efficiency is summarized in Table 3.[110] Nickel can be deposited but Mo cannot be deposited by itself. Therefore, Ni may be more noble than Mo. On the other hand, Mo content in the alloys was increased by such an alternation of the magnitude of plating variables as an increase in total metal concentration in bath, a decrease in current density and an increase in bath temperature, as shown in Table 3. In the electrodeposition of alloys, the content of more noble metal is increased by the alternation of plating variables which prevent the decrease in the metal ion concentration in the cathode diffusion layer. In this case, Mo acts as the more noble metal than Ni. Thus, the electrodeposition behavior of Mo (W)–iron-group metal alloys cannot be explained by the common theory of alloy deposition.

The mechanism of induced codeposition proposed up to about 1960 was summarized by Brenner.[111] In the codeposition mechanism proposed so far, hypotheses have been advanced on the basis of the formation of insoluble intermediate compound of partly reduced Mo (W) oxide.

The existence of intermediate oxide was first suggested

Fig. 7. Relationship between alloy composition and cathode pontential in electrodeposition of Zn–Ni alloys.[85]

Table 3. Effect of increase in magnitude of plating variables on Mo content in alloys and on cathode current efficiency during electrodeposition of Ni–Mo alloys.[110]

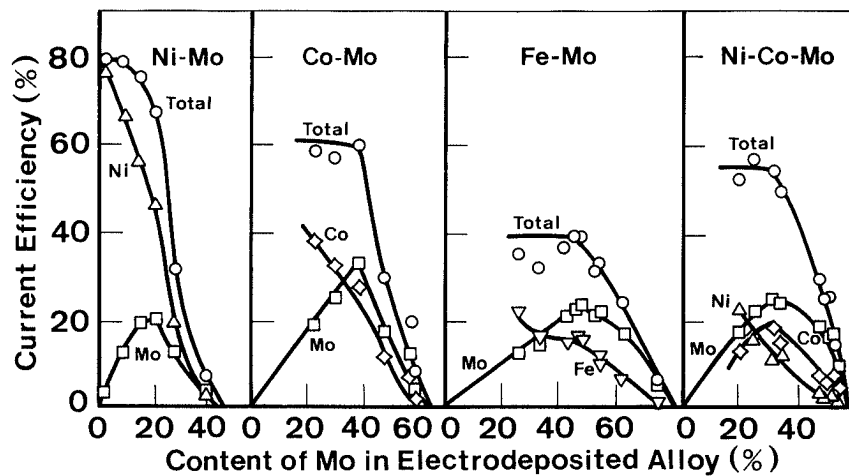| Plating variable	Range examined	Mo % in deposit	Current efficiency
Metal % of Mo in bath	$0 \rightarrow 50\%$	Increase	Decrease
Total metal concentration	$0.05 \rightarrow 0.70$ mol/L	Increase	Decrease
pH	$10.5 \rightarrow 12.5$	Decrease	Increase
Current density	$100 \rightarrow 2000$ A/m^2	Decrease	Increase
Temperature	$30 \rightarrow 70°C$	Increase	Slightly increase

Fig. 8.

Relationship between alloy composition and cathode current efficiency during electrodeposition of Mo–iron-group metal alloys.[121]

in the electrodeposition of W–iron-group metal alloys by Holt et al.[112−114] Ernst and Holt[115] then proposed that the reduction of molybdate ion in ammoniacal citrate solutions was accomplished in the following two steps: (1) electrochemical formation of the intermediate lower Mo oxide and (2) reduction of this oxide film by atomic hydrogen which was held on the freshly deposited inducing iron-group metals utilizing their unpaired electrons. Sastry[116] discussed the effect of addition agent on the electrodeposition behavior of W–iron-group metal alloys, and pointed out that selenious acid as well as S-compounds such as thiourea, thiosulfate and thiocyanate inhibited the deposition of W. It was estimated that there was no free electrons to hold hydrogen which brought about the initial reduction of W oxide or hydroxide since the unpaired electrons of inducing metal were utilized by those of S or Se atoms to form covalent bond.

Electrodeposition behavior of Mo–iron-group metal alloys from ammoniacal tartrate solutions was investigated in detail by Higashi and Fukushima et al.[117−123] Using the stationary electrode polarographic technique, the effect of S- and N-compounds on the Ni deposition was compared with that of molybdate ions. It was shown that the adsorbed molybdate ion caused the depolarization of iron-group metal.[122] Further, the relationship between the composition of electrodeposited alloys and the cathode current efficiency indicated the two characteristic alloy compositions: the one appeared at a maximum partial current efficiency of Mo and the other corresponded to the limiting content of Mo (Fig. 8). These two compositions were in good agreement with the calculated ones based on the number of unpaired $3d$ electrons of iron-group metals, suggesting that the Mo^{4+} oxide electrochemically formed was reduced by atomic hydrogen[121] held on freshly deposited iron-group metal. The valence state of Mo in the intermediate oxide was also confirmed by XPS study.[123]

Imanaga et al. conducted the electrodeposition of Ni–Mo alloys from ammoniacal citrate solutions to investigate the effect of plating variables,[124−126] alkaline cations[127] and addition agents[128] on the electrodeposition behavior. He also studied the complex formation of Ni and Mo ions in the electrolytes[129] and single

deposition behavior of Mo.[130] In their latest publications,[131,132] MoO_2 was detected by X-ray diffraction and XPS in both deposits obtained from the alloy plating bath and single molybdate bath. It was estimated that the intermediate MoO_2 was reduced by hydrogen bonded with d-band valency of Ni. The Mo content of the alloys obtained at higher current efficiencies was related to the number of d-band valency of iron-group metal, and the alloys would lose all d-band valency when the maximum Mo content, corresponding to the composition Ni_4Mo, was attained.

Using simple sulfate solutions, Golubkov and Yur'ev[133] investigated the ternary Mo–Fe–Ni alloy deposition. In the mechanism suggested, the formation of trivalent Mo oxide film, which was permeable to Fe^{2+} and Ni^{2+} ions, primarily occurred to weaken the Mo–O chemical bond owing to the formation of additional bonds of Mo with Fe and Ni. This favored the reduction of Mo to the metal, resulting in the formation of corresponding alloy. In addition to this, the decrease in Mo activity, which was resulted from the alloy formation, facilitated the reduction of Mo. This hypothesis was recently supported by Tereszko et al.,[134] who measured the polarization curves for Mo–Ni alloy deposition onto the rotating disk electrode from ammoniacal citrate solutions.

Amorphous Co–Mo alloys were electrodeposited using pulsating current from acid citrate solutions.[108] It was found that Tafel slope of the prewave in the polarization curve for alloy deposition was significantly large. This suggested the existence of insoluble resistive films on the cathode. This film was supposed to be adsorbed hydrated Mo–Co complex, corresponding to the composition $CoO \cdot xMoO_2 \cdot yH_2O$, which was reduced electrochemically at potentials more positive than for Co single deposition.

Chassaing et al.[135] investigated the Mo–Ni alloy deposition from ammoniacal citrate solutions by means of a.c. impedance measurement coupled with AES and EDAX analysis. They also insisted the existence of complex oxide, MoO_2Ni_4, on the cathode, which was resulted from the transformation of MoO_2 in the presence of Ni^{2+}, although no data were available on the species which underwent reduction.

The hypothetic mechanism including the formation of the complex Ni_x–Mo_y oxide on the cathode was presented in the pyrophosphate solutions by Degrez and Winand[136] who also suggested that the adsorbed molybdate ion inhibited the Ni deposition at more positive potentials than that of alloy deposition.

On the other hand, several hypotheses, in which the formation of insoluble Mo oxide was not assumed, have been proposed. One of such mechanisms was based on the complexation between W (Mo) ion and the ions of iron-group metal.[137,138] A complex ion containing both W (Mo) and iron-group metal was formed in solution and its discharge made the simultaneous deposition of both metals possible. Afterward, the formation of such complex ions was suggested by Clark and Lietzke[139] using absorption spectrometry and Sallo and Fisher[140] also discussed the effect of additive S-compounds on W–Ni alloy deposition in relation to the complex ion formation. This mechanism was, however, criticized by Imanaga[128,129] and Shiio et al.[141] using spectrophotometric technique, who showed no existence of such a polynuclear complex in ammoniacal citrate and tartrate solutions.

The hypothesis of the polarization transfer was advanced by Brenner.[142] W is restrained from deposition kinetically in acid solutions and thermodynamically in alkaline solutions. The polarization energy of inducing metal was provided as the activation energy in former case and as the deficiency of free energy required for the deposition in latter case. Therefore, the deposition of the iron-group metal was the primary factor that determined the current density–potential relations of codeposition. This hypothesis was supported by Singh et al.[143] recently in the deposition of ternary W–Ni–Co alloys.

According to the oscillographic study of W–Ni alloy deposition by Frantsevich-Zabudovskaya et al.,[144, 145] Ni ion reduced electrochemically to form activated Ni metal. A part of electrons belonging to activated Ni was then given to tungstate ion to bring about the formation of activated complex ion containing both Ni and W. This complex was reduced by electron from the electrode, forming the solid solution of Ni and W.

On the basis of the fact that the deposition potential of alloys are more positive than those of iron-group metals, Yur'ev et al.[133,146] suggested that the thermodynamical depolarization caused by a decrease in activity of metal due to alloy formation allowed the codeposition of Mo or W. They insisted that the formation of intermetallic compound, Co_3W, found in the deposition of W–Co alloys from ammoniacal citrate solutions caused the large depolarization to make possible the codeposition of W with iron-group metal.

Omi and Yamamoto[99–103,147,148] actively made an approach to the mechanism of the induced electrodeposition of Mo, W or P alloys from the standpoint of microstructure of the alloys. They proposed the structural model for Co–W alloy, for example, consisting of close packed tetrahedra, each composed of three Co atoms and one W atom. Interference functions calculated from the above model agreed well with X-ray diffraction data of the alloys. The atomic arrangement in the model

formed distorted icosahedra which forbade crystallinity in the alloys, indicating that they had nonequilibrium structures and then the thermodynamic depolarization[133,146] was not expected. It was concluded that W was able to deposit only at the sites on n-atoms cluster of iron-group metal.

3.2. P–Iron-group Metal System

Since the electrodeposited P–iron-group metal alloys often show amorphous structure, the number of reports increases recently on the electrodeposition of the alloys, especially in the fields of the mechanism of the amorphous phase formation as well as the crystallization process with heat treatment. It is beyond the scope of this review to discuss the structure of Ni–P deposits and readers are referred to monographs or other reviews.[98,148–158]

To overcome the shortcomings of electroless Ni–P plating such as an expensive reducing agent, a high operating temperature and difficulty in controlling of deposition rate, Brenner et al.[159] developed the electrolytes for the electrodeposition of Ni–P and Co–P alloys (Table 4), and classified the codeposition of P with iron-group metals into induced codeposition.[160] Watts-type solutions of pH 1 were used, to which phosphorous and phosphoric acids were added as a P supplier to the deposits and as a buffering agent, respectively. High acidity of the plaiting solutions was required not only to prevent basic compounds from precipitation, but also to permit the phosphorous ion to exist stably from which P was depositable. Brenner suggested that, because of the appreciable heat of formation of the phosphides of Co and Ni, the decrease in free energy resulting from the alloy formation shifted the equilibrium potential of P to more positive potentials. However, this potential shift was not critical factor, since P was thermodynamically capable of being reduced from phosphorous acid at potentials attainable in aqueous solution.

Using the similar type solutions as Brenner, Narayan and Mungole[161] proposed the reduction process through hypophosphite to explain the effect of various plating variables in Ni–P alloy deposition.

Using direct and pulsating current, Ni–P alloys were electrodeposited also from the similar type of solutions by Ratzker et al.[162] The cathodic reactions were believed
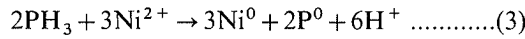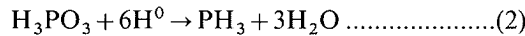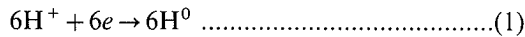
Table 4. Typical electrolysis conditions for Ni–P alloys of high-P type.[160]

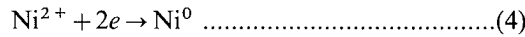| Bath composition		Operating conditions and bath performance	
$NiSO_4 \cdot 6H_2O$	0.57 mol/L	Current density	0.5–4 kA/m²
$NiCl_2 \cdot 6H_2O$	0.19 mol/L	Temperature	75–95°C
Ni added as		Current efficiency	50%
phosphate or	0.24 mol/L	P content	12–15%
phosphite*		in deposit	
H_3PO_4	0.5 mol/L	Type of	Bright, strong,
H_3PO_3	0.5 mol/L	deposit	brittle
pH	0.5–1		

* Part of Ni content of the bath was introduced as a solution of nickel phosphite or nickel phosphate of pH about 1.0. This solution was formed by partially neutralizing with nickel carbonate the phosphorous and phosphoric acid required for the bath.

to consist of both direct and indirect processes described below.
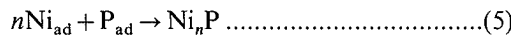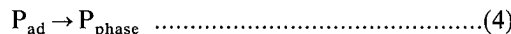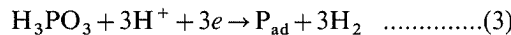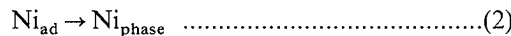
Indirect reduction:

$$6H^+ + 6e \rightarrow 6H^0 \quad\text{.................................(1)}$$

$$H_3PO_3 + 6H^0 \rightarrow PH_3 + 3H_2O \quad\text{...................(2)}$$

$$2PH_3 + 3Ni^{2+} \rightarrow 3Ni^0 + 2P^0 + 6H^+ \quad\text{...........(3)}$$

Direct reduction:

$$Ni^{2+} + 2e \rightarrow Ni^0 \quad\text{....................................(4)}$$

$$2H^+ + 2e \rightarrow H_2 \quad\text{...(5)}$$
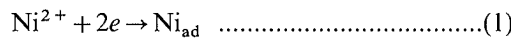
It was insisted that elemental P was incorporated in Ni lattice to prevent normal crystal growth, resulting in a fine-grained or even an amorphous alloy formation if sufficient P was present. Further, the slow diffusion rate of phosphorous acid, because of its large size, accounted for the facts that the P content was greater at lower current densities and that pulsed current increased P content by relaxing the diffusion layer to allow phosphorous acid to approach the cathode.

In the paper describing the pulse plating behavior of Ni–P alloys from Watts-type solutions containing phosphorous acid by Ohno et al.,[163] the feature of the cathodic reaction was explained using the generalized equations written in following forms:

$$Ni^{2+} + 2e \rightarrow Ni_{ad} \quad\text{.....................................(1)}$$

$$Ni_{ad} \rightarrow Ni_{phase} \quad\text{..(2)}$$

$$H_3PO_3 + 3H^+ + 3e \rightarrow P_{ad} + 3H_2 \quad\text{..............(3)}$$

$$P_{ad} \rightarrow P_{phase} \quad\text{..(4)}$$

$$nNi_{ad} + P_{ad} \rightarrow Ni_nP \quad\text{...................................(5)}$$

where the subscripts of ad and phase designated adsorbed state and solid phase, respectively.

As step (3) was enhanced by hydronium ion, a low-pH plating bath was preferable for obtaining alloys. Since step (4) was thermodynamically prohibited, step (3) proceeded only when it occurred together with reaction (1), forming alloys as shown in reaction (5). Watanabe and Kanayama[164] also mentioned that the fact that the alloys of higher P content were obtained at lower current densities was not explainable if the alloy formation followed the steps presented by Ohno et al.[163] They insisted that elemental P (or PH_3^{2+}) liberated by step (3) adsorbed on the deposited Ni. Therefore, the relative amount of adsorbed P on Ni became higher to bring about the formation of P-rich alloys while the rate of Ni deposition was lower at lower current densities. On the other hand, this variation of P content in deposits with current density was explained in terms of pH rise in the cathode layer due to hydrogen evolution during electrolysis.[165]

For the electrodeposition process of amorphous Ni–P and Ru–Ni–P alloys on the rotating disk electrode, Chen and White[166,167] developed a mathematical model including mass transport equation, Butler–Volmer's kinetic rate expression and the molar fractions of individual component in the solid state, and indicated that the model predicted well the electrodeposition behavior. In their study, the hypophosphorous acid was assumed to be produced in the electrochemical reduction of phosphorous and phosphoric acid, which was followed by the deposition of elemental P.[166]

Besides the characteristic features of the electrodeposition of Ni–P alloys as mentioned above, it is known that banded structure is observed in the cross sections of deposited alloys. The development of such structure was attributed to the variation of P content caused by the pH change in the cathode layer.[159,162,168,169]

Practical use of electrodeposited alloys has been rather limited so far because of the difficulty of establishing the operating conditions which permitted the stable deposition of alloys of fixed composition. In recent years, the electrodeposition of alloys has aroused an intense interest as a new technique which has great industrial possibilities for producing the coatings of higher quality in the field of surface finishing as well as for the hydrometallurgical production of advanced materials such as intermetallic compounds, supersaturated solid solutions and amorphous alloys which cannot be obtained pyrometallurgically. The electrodeposition of iron-group metal alloys is important both in industrial and academic senses, whereas the mechanism of the alloy deposition is still in an incomplete stage as shown in this present review. Efforts to clarify the mechanism will lead to the promotion of the application of alloy deposition in many fields of industry.

The figures are reprinted by permission of the publishers, The Electrochemical Society, Inc., The Surface Finishing Society of Japan and The Electrochemical Society of Japan.

REFERENCES

1) A. Krohn and C. W. Bohn: Electrodeposition Surf. Treat., 1 (1972/73), 119.
2) G. J. Rudzki: Surface Finishing System, Finishing Publ., (1983), 60.
3) T. Hada: Proc. Int. Conf. Zinc and Zinc Alloy Coated Steel, ISIJ, Tokyo, (1989), 111.
4) T. Mottae: Proc. Int. Conf. Zinc and Zinc Alloy Coated Steel, ISIJ, Tokyo, (1989), 625.
5) T. Watanabe, Y. Shindou, T. Shiota, K. Yamato and S. Monura: Proc. Int. Conf. Zinc and Zinc Alloy Coated Steel, ISIJ, Tokyo, (1989), 80.
6) R. J. Clauss, R. A. Tremmel and R. W. Klein: Trans. Inst. Met. Finish., 53 (1975), No. 1, 22.
7) B. Garner: Prod. Finish., 29 (1976), No. 9, 20.
8) T. Koga: Jitsumu Hyomen Gijutsu (Met. Finish. Pract.), (1976), No. 263, 535.
9) R. J. Clauss and R. A. Tremmel: World Congr. Met. Finish., 9th., Int. Union for Electrodeposition and Surf. Finish., Amsterdam, (1976), 901.
10) L. Free: Prod. Finish., 30 (1977), No. 5, 12.
11) T. Koga: Met. Technol., 49 (1979), No. 5, 46.
12) J. S. Hadley and J. O'Grady: Trans. Inst. Met. Finish., 59 (1981), No. 3, 89.
13) R. A. Tremmel: Plat. Surf. Finish., 68 (1981), No. 1, 22.
14) R. A. Tremmel: Plat. Surf. Finish., 68 (1981), No. 2, 30.
15) R. J. Clauss: ASTM Spec. Tech. Publ., No. 767, (1982), 214.
16) Y. Suzuki, M. Izumiya and O. Asai: J. Met. Finish. Soc. Jpn., 28 (1977), 513.
17) Y. Kamo and G. Otomo: Res. Rep. Fac. Eng. Tohoku Gakuin Univ., 15 (1980), 27.

18) P. Duke, T. Montelbano and L. Missel: *Plat. Surf. Finish.*, **69** (1982), No. 9, 61.

19) I. M. Croll and L. T. Romankiw: Proc. Symp. Electrodeposition Technol. Theory Pract., Electrochem. Soc., San Diego, 1986, (1987), 285.

20) S. S. Djokic, M. D. Maksimovic and D. C. Stefanovic: *J. Appl. Electrochem.*, **19** (1989), 802.

21) R. L. White: *Plat. Surf. Finish.*, **75** (1988), No. 4, 70.

22) Y. Omata, K. Kanai and N. Kaminaka: *J. Met. Finish. Soc. Jpn.*, **34** (1983), 309.

23) Y. Kamo: *Res. Rep. Fac. Eng. Tohoku Gakuin Univ.*, **20** (1986), 165.

24) O. Muller, G. Scilla and R. Fernquist: *Thin Solid Films*, **117** (1984), 281.

25) S. N. Srimathi and S. M. Mayanna: *Mater. Chem. Phys.*, **11** (1984), 351.

26) H. Dahms: *J. Electroanal. Chem.*, **8** (1964), 5.

27) H. Dahms and I. M. Croll: *J. Electrochem. Soc.*, **112** (1965), 771.

28) J. Bielinski and J. Przyluski: *Surf. Technol.*, **9** (1979), 53.

29) E. Beltowska-Lehman and A. Riesenkampf: *Surf. Technol.*, **11** (1980), 349.

30) J. Horkans: *J. Electrochem. Soc.*, **126** (1979), 1861.

31) J. Horkans: *J. Electrochem. Soc.*, **128** (1981), 45.

32) N. Koura and N. Yasuda: *Denki Kagaku*, **49** (1981), 371.

33) N. Yasuda and N. Koura: *J. Met. Finish. Soc. Jpn.*, **33** (1982), 427.

34) N. Nakamura and T. Hayashi: *Plat. Surf. Finish.*, **72** (1985), No. 8, 42.

35) S. N. Srimathi, B. S. Sheshadri and S. M. Mayanna: *Surf. Technol.*, **17** (1982), 217.

36) D. L. Grimmett, M. Schwartz and K. Nobe: *J. Electrochem. Soc.*, **137** (1990), 3414.

37) L. T. Romankiw: Proc. Symp. Electrodeposition Technol. Theory Pract., Electrochem. Soc., San Diego, 1986, (1987), 301.

38) J. Bielinski and J. Przyluski: *Surf. Technol.*, **9** (1979), 65.

39) S. Hessami and C. W. Tobias: *J. Electroctrochem. Soc.*, **136** (1989), 3611.

40) J. O'M. Bockris, D. Drazic and A. R. Despic: *Electrochim. Acta*, **4** (1961), 325.

41) J. Matulis and R. Slizys: *Electrochim. Acta*, **9** (1964), 1177.

42) P. C. Andricacos, C. Arana, J. Tabib, J. Dukovic and T. Romankiw: *J. Electrochem. Soc.*, **136** (1989), 1336.

43) S. Biallozor and M. Lieder: *Surf. Technol.*, **21** (1984), 1.

44) M. Lieder and S. Biallozor: *Surf. Technol.*, **26** (1985), 23.

45) G. H. Cocket and E. S. Spencer-Timms: *J. Electrochem. Soc.*, **108** (1961), 906.

46) M. E. Henstock and E. S. Spencer-Timms: *Trans. Inst. Met. Finish.*, **40** (1963), 179.

47) W. O. Freitag, J. S. Mathias and G. Diguilio: *J. Electrochem. Soc.*, **111** (1964), 35.

48) H. Dahms: *Electrochem. Technol.*, **4** (1966), 530.

49) D. R. Eastham, P. J. Boden and M. E. Henstock: *Trans. Inst. Met. Finish.*, **46** (1968), 37.

50) I. Ohno: *J. Met. Finish. Soc. Jpn.*, **23** (1972), 163.

51) F. H. Edelman: *J. Electrochem. Soc.*, **109** (1962), 440.

52) A. Brenner: Electrodeposition of Alloys, Vol. 2, Academic Press, New York and London, (1963), 221.

53) A. Knoedler: Metalloberflaeche, **21** (1967), 321.

54) E. Raub, A. Knoedler, A. Disam and H. Kawase: *Metalloberflaeche*, **23** (1969), 293.

55) K. Knoedler: *Surf. Technol.*, **4** (1976), 441.

56) E. Raub: *Plat. Surf. Finish.*, **63** (1976), No. 2, 29.

57) H. Ito, K. Higashi and H. Sato: *J. Met. Finish. Soc. Jpn.*, **20** (1969), 149.

58) H. Ito, K. Higashi and H. Sato: *J. Met. Finish. Soc. Jpn.*, **20** (1969), 595.

59) K. Higashi, H. Fukushima, T. Urakawa, T. Adaniya and K. Matsudo: *J. Electrochem. Soc.*, **128** (1981), 2081.

60) H. Fukushima, T. Akiyama, J.-H. Lee, M. Yamaguchi and K. Higashi: *J. Met. Finish. Soc. Jpn.*, **33** (1982), 574.

61) T. Adaniya, H. Fukushima and K. Higashi: *Tetsu-to-Hagané*, **69** (1983), 959.

62) H. Fukushima, T. Akiyama, K. Kakihara, T. Adaniya and K.

63) T. Akiyama, L. Li, H. Fukushima, K. Higashi and T. Hara: *Tetsu-to-Hagané*, **74** (1988), 130.

64) H. Fukushima, T. Akiyama, K. Higashi, R. Kammel and M. Karimkhani: *Metall*, **42** (1988), 242.

65) H. Fukushima: Proc. Int. Conf. Zinc and Zinc Alloy Coated Steel, ISIJ, Tokyo, (1989), 19.

66) T. Akiyama, H. Fukushima, K. Higashi, M. Karimkhani and R. Kammel: Proc. Int. Conf. Zinc and Zinc Alloy Coated Steel, ISIJ, Tokyo, (1989), 45.

67) T. Akiyama, H. Fukushima, K. Higashi, M. Sagiyama and R. Kammel: *Metall*, **43** (1989), 1142.

68) H. Fukushima, T. Akiyama, K. Higashi, R. Kammel and˙M. Karimkhani: *Metall*, **44** (1990), 754.

69) A. Shibuya and T. Kurimoto: *J. Met. Finish. Soc. Jpn.*, **33** (1983), 544.

70) A. R. Fajardo, R. Winand, A. Weymeersch and L. Renard: AESF 5th. Continuous Strip Plat. Symp., Am. Electroplaters' Soc., Dearborn, (1987), S1.

71) K. Higashi, Y. Hayashi, H. Fukushima, T. Akiyama and H. Hagi: A Fundamental Study of Corrosion-Resistant Zinc–Nickel Electroplating, NiDI Techinical Series No. 10036, Nickel Development Inst., Toronto, (1990), 43.

72) Y. Tsuru, S. Tashiro, T. Tanaka, K. Hosokawa: *J. Met. Finish. Soc. Jpn.*, **42** (1991), 105.

73) T. Watanabe, M. Ohmura, A. Tonouchi, T. Honma and T. Adaniya: *J. Met. Finish. Soc. Jpn.*, **33** (1982), 531.

74) A. Komada, A. Matsuda, T. Yoshihara and H. Kimura: AES 4th. Continuous Strip Plat. Symp., Am. Electroplaters' Soc., Chicago, (1984), C1.

75) T. Irie, K. Kyono, H. Kimura, T. Honjo, K. Yamato, T. Ishihara and A. Matsuda: AES 4th. Continuous Strip Plat. Symp., Am. Electroplaters' Soc., Chicago, (1984), G1.

76) B. P. Yur'ev and L. V. Volkov: *Zh. Prikl. Khim.*, **38** (1963), 66.

77) L. Felloni, R. Fratesi, E. Quadrini and G. Roventi: *J. Appl. Electrochem.*, **17** (1987), 574.

78) M. J. Nicol and H. I. Philip: *J. Electroanal. Chem.*, **70** (1976), 233.

79) M. F. Mathias and T. W. Chapman: Energy Reduct. Tech. Met. Electrochem. Processes, Metall. Soc. AIME, New York, (1985), 163.

80) M. F. Mathias and T. W. Chapman: *J. Electrochem. Soc.*, **134** (1987), 1408.

81) M. F. Mathias and T. W. Chapman: *J. Electrochem. Soc.*, **137** (1990), 102.

82) M. F. Mathias and T. W. Chapman: *J. Appl. Electrochem.*, **20** (1990), 1.

83) M. Kurachi and K. Fujiwara: *Denki Kagaku*, **38** (1970), 600.

84) Y. Imai and M. Kurachi: *Denki Kagaku*, **45** (1977), 728.

85) Y. Imai, T. Watanabe and M. Kurachi: *Denki Kagaku*, **46** (1978), 202.

86) Y. Imai, S. Ohsumi and M. Kurachi: *Denki Kagaku*, **46** (1978), 264.

87) Y. Imai and M. Kurachi: *Denki Kagaku*, **47** (1979), 89.

88) M. Kurachi and A. Sakoda: *J. Met. Finish. Soc. Jpn.*, **31** (1980), 512.

89) T. Kurashige and A. Shibuya: *J. Met. Finish. Soc. Jpn.*, **37** (1986), 55.

90) S. Swathirajan: *J. Electrochem. Soc.*, **133** (1986), 671.

91) S. Swathirajan: *J. Electrochem. Soc.*, **134** (1987), 211.

92) Von J. Francyk and T. Zolnierczyk: *Metalloberflaeche*, **34** (1980), 6.

93) J. K. Dennis, K. J. Lodge and F. A. Still: *Trans. Inst. Met. Finish.*, **55** (1977), 17.

94) J. K. Dennis and D. Jones: *Tribol. Int.*, **14** (1981), 271.

95) M. Kamada, M. Yoshida, K. Kanechika and F. Yamamoto: *J. Met. Finish. Soc. Jpn.*, **36** (1985), 5.

96) W. L. Wade Jr. and G. Sands: *J. Electrochem. Soc.*, **118** (1971), 1137.

97) W. O. Freitag and J. S. Mathias: *J. Electrochem. Soc.*, **112** (1965), 64.

98) T. Masumoto and T. Watanabe: Amorufasmekkihou to sono ouyou (in Japanese), Nikkan Kogyo Shinbun-sha, Tokyo, (1990).

99) T. Omi, H. Yamamoto and H. L. Glass: *J. Electrochem. Soc.*, **119** (1972), 168.

100) T. Omi, H. L. Glass and H. Yamamoto: *J. Electrochem. Soc.*, **123** (1976), 341.

101) T. Omi and H. Yamamoto: *J. Met. Finish. Soc. Jpn.*, **29** (1978), 455.

102) T. Omi and H. Yamamoto: *J. Met. Finish. Soc. Jpn.*, **29** (1978), 460.

103) T. Omi, M. Hiramatsu, S. Hanada and H. Yamamoto: *J. Met. Finish. Soc. Jpn.*, **31** (1980), 85.

104) M. Yanagihara: *J. Met. Finish. Soc. Jpn.*, **29** (1978), 636.

105) T. Watanabe and Y. Tanabe: Proc. Int. Conf. Rapidly Quenched Met., 5th., Met. Soc., Brighton, 1 (1984), 127.

106) U. Admon, P. Dariel and E. Gruenbaum: *J. Phys. Chem.*, **59** (1986), 2002.

107) S. Yao and M. Kowaka: *J. Met. Finish Soc. Jpn.*, **39** (1988), 736.

108) Y. Jyoko, I. Ohno and S. Haruyama: *J. Jpn. Inst. Met.*, **52** (1988), 95.

109) T. Watanabe, T. Naoe, A. Mitsuo and S. Katsumata: *J. Surf. Finish. Soc. Jpn.*, **40** (1989), 458.

110) H. Fukushima and K. Higashi: *J Met. Finish. Soc. Jpn.*, **29** (1978), 627.

111) A. Brenner: Electrodeposition of Alloys, Vol. 2, Academic Press, New York and London, (1963), 399.

112) M. L. Holt and M. L. Nielsen: *Trans. Electrochem. Soc.*, **82** (1942), 193.

113) M. L. Holt and R. E. Black: *Trans. Electrochem. Soc.*, **82** (1942), 205.

114) M. L. Nielsen and M. L. Holt: *Trans. Electrochem. Soc.*, **82** (1942), 217.

115) D. W. Ernst and M. L. Holt: *J. Electrochem. Soc.*, **105** (1958), 686.

116) D. S. R. Sastry: *Met. Finish.*, **63** (1965), No. 11, 86.

117) K. Higashi and H. Fukushima: *J. Met. Finish. Soc. Jpn.*, **24** (1973), 486.

118) K. Higashi, H. Fukushima, H. Ohashi and T. Akiyama: *J. Met. Finish. Soc. Jpn.*, **27** (1976), 590.

119) K. Higashi, H. Fukushima and K. Kitamura: *J. Met. Finish. Soc. Jpn.*, **28** (1977), 112.

120) K. Higashi, H. Fukushima and M. Kanda: *J. Min. Metall. Inst. Jpn.*, **92** (1976), 561.

121) H. Fukushima, T. Akiyama, S. Akagi and K. Higashi: *Trans. Jpn. Inst. Met.*, **20** (1979), 358.

122) H. Fukushima, T. Akiyama, H. Nakakoji and K. Higashi: *J. Met. Finish. Soc. Jpn.*, **30** (1979), 600.

123) H. Fukushima, T. Akiyama and K. Higashi: *J. Met. Finish. Soc. Jpn.*, **32** (1981), 58.

124) H. Imanaga: *J. Chem. Soc. Jpn. (Ind. Chem. Sect.)*, **63** (1960), 1336.

125) H. Imanaga: *J. Chem. Soc. Jpn. (Ind. Chem. Sect.)*, **67** (1964), 282.

126) H. Imanaga: *J. Chem. Soc. Jpn. (Ind. Chem. Sect.)*, **67** (1964), 803.

127) H. Imanaga: *J. Chem. Soc. Jpn. (Ind. Chem. Sect.)*, **66** (1963), 1639.

128) H. Imanaga: *J. Chem. Soc. Jpn. (Ind. Chem. Sect.)*, **67** (1964), 286.

129) H. Imanaga: *J. Chem. Soc. Jpn. (Ind. Chem. Sect.)*, **66** (1963), 1792.

130) T. Komura and H. Imanaga: *J. Chem. Soc. Jpn. (Ind. Chem. Sect.)*, **71** (1968), 827.

131) S. Rengakuji, K. Nishibe, Y. Nakamura and H. Imanaga: *Denki Kagaku*, **58** (1990), 63.

132) S. Rengakuji, Y. Nakamura, M. Inoue, K. Nishibe and H. Imanaga: *Denki Kagaku*, **59** (1991), 885.

133) L. A. Golubkov and B. P. Yur'ev: *Zh. Prikl. Khim.*, **44** (1971), 2419.

134) B. Tereszko, A. Riesenkampf and K. Vu Quang: *Surf. Technol.*, **12** (1981), 301.

135) E. Chassaing, K. Vu Quang and R. Wiart: *J. Appl. Electrochem.*, **19** (1989), 839.

136) M. Degrez and R. Winand: *Oberflaeche-Surf.*, **31** (1990), No. 8, 8.

137) M. L. Holt: *Trans. Electrochem. Soc.*, **71** (1937), 301.

138) L. E. Vaaler and M. L. Holt: *Trans. Electrochem. Soc.*, **88** (1946), 43.

139) W. L. Clark and M. H. Lietzke: *J. Electrochem. Soc.*, **99** (1952), 245.

140) J. S. Sallo and D. Fisher: *J. Electrochem. Soc.*, **107** (1960), 277.

141) H. Shiio and T. Shimizu: *J. Met. Finish. Soc. Jpn.*, **20** (1969), 105.

142) A. Brenner: Electrodeposition of Alloys, Vol. 2, Academic Press, New York and London, (1963), 404.

143) V. B. Singh, L. C. Singh and P. K. Tikoo: *J. Electrochem. Soc.*, **127** (1980), 590.

144) T. F. Frantsevich-Zabludovskaya, A. I. Zayats and V. T. Barchuk: *Ukr. Khim. Zh.*, **25** (1959), 713.

145) T. F. Frantsevich-Zabludovskaya, A. I. Zayats and V. T. Barchuk: *Ukr. Khim. Zh.*, **26** (1960), 10.

146) B. P. Yur'ev, L. S. Kiseleva and I. B. Zabelin: *Zh. Prikl. Khim.*, **45** (1971), 85.

147) T. Omi, M. Nakamura and Y. Yamamoto: *J. Met. Finish. Soc. Jpn.*, **39** (1988), 809.

148) T. Omi: *J. Surf. Finish. Soc. Jpn.*, **40** (1989), 368.

149) H. Yamamoto and T. Omi: *J. Met. Finish. Soc. Jpn.*, **31** (1980), 294.

150) T. Watanabe: *Jitsumu Hyomen Gijutsu (Met. Finish. Pract.)*, **32** (1985), 544.

151) T. Watanabe: *J. Met. Finish. Soc. Jpn.*, **38** (1987), 210.

152) T. Watanabe: *Tetsu-to-Hagané*, **73** (1987), 2180.

153) M. Ogata: *J. Met. Finish. Soc. Jpn.*, **39** (1988), 169.

154) T. Watanabe: *J. Surf. Finish. Soc. Jpn.*, **40** (1989), 375.

155) T. Watanabe: *J. Surf. Finish. Soc. Jpn.*, **40** (1989), 494.

156) T. Watanabe: *Met. Technol.*, **60** (1990), No. 6, 2.

157) M. Kowaka and Y. Ruan: *Met. Technol.*, **60** (1990), No. 6, 8.

158) T. Watanabe and Y. Shimizu: *Tetsu-to-Hagané*, **76** (1990), 1597.

159) A. Brenner, D. E. Couch and E. K. Williams: *J. Res. Natl. Bur. Stand.*, **44** (1950), 109.

160) A. Brenner: Electrodeposition of Alloys, Vol. 2, Academic Press, New York and London, (1963), 457.

161) R. Narayan and N. Mungole: *Surf. Technol.*, **24** (1985), 233.

162) M. Ratzker, D. S. Lashmore and K. W. Pratt: *Plat. Surf. Finish.*, **73** (1986), No. 9, 74.

163) I. Ohno, H. Ohfuruton and S. Haruyama: *J. Jpn. Inst. Met.*, **50** (1986), 1075.

164) T. Watanabe and T. Kanayama: *J. Surf. Finish. Soc. Jpn.*, **40** (1989), 425.

165) A. Kawashima, Y.-P. Lu, H. Habazaki, K. Asami and K. Hashimoto: *Boshoku Gijutsu (Corros. Eng.)*, **38** (1989), 593.

166) S. Chen and R. E. White: Proc. Symp. Electrodeposition Technol. Theory Pract., Electrochem. Soc., San Diego, 1986, (1987), 499.

167) S. Chen, K.-M. Yin and R. E. White: *J. Electrochem. Soc.*, **135** (1988), 2193.

168) C. C. Nee and R. Weil: *Surf. Techonol.*, **25** (1985), 7.

169) K. Shimizu, K. Kobayashi, G. E. Thompson and G. C. Wood: *J. Surf. Finish. Soc. Jpn.*, **42** (1991), 122.